Nucleophilic Addition of CH, NH, and OH Bonds to the Phosphadiazonium Cation and Interpretation of ^{31}P Chemical Shifts at Dicoordinate Phosphorus Centers

Neil Burford,* T. Stanley Cameron,* Jason A. C. Clyburne, Klaus Eichele, Katherine N. Robertson, Sergey Sereda, Roderick E. Wasylishen,* and W. Alex Whitla[1]

Department of Chemistry, Dalhousie University, Halifax, Nova Scotia B3H 4J3, Canada

Received February 8, 1996[⊗]

The phosphadiazonium cation $[Mes^*NP]^+$ reacts quantitatively with the fluorenylide anion, Mes^*NH_2, and Mes*OH (Mes* = 2,4,6-tri-*tert*-butylphenyl), resulting in formal insertion of the N−P moiety into the H−Y (Y = C, N, O) bonds. Specifically, reaction of Mes*NPCl with fluorenyllithium gives the aminofluorenylidenephosphine [crystal data: $C_{31}H_{38}NP$, monoclinic, $P2_1/c$, a = 9.568(8) Å, b = 24.25(2) Å, c = 11.77(1) Å, β = 101.38(8)°, Z = 4]. Similarly, reaction of $[Mes^*NP][GaCl_4]$ with Mes^*NH_2 gives the diaminophosphenium salt [Mes*N(H)PN(H)Mes*][$GaCl_4$] [crystal data: $C_{36}H_{60}Cl_4GaN_2P$, monoclinic, $C2/c$, a = 24.921(2) Å, b = 10.198(4) Å, c = 16.445(2) Å, β = 93.32(1)°, Z = 4], and reaction with Mes*OH gives the first example of an aminooxyphosphenium salt [Mes*N(H)POMes*][$GaCl_4$]. It is proposed that the reactions involve nucleophilic attack at phosphorus followed by a 1,3-hydrogen migration from Y to N. Experimental evidence for the formation of σ-complex intermediates is provided by the isolation of $[Mes^*NP{-}PPh_3][SO_3CF_3]$ [crystal data: $C_{37}H_{44}F_3NO_3P_2S$, triclinic, $P\bar{1}$, a = 10.663(1) Å, b = 19.439(1) Å, c = 10.502(1) Å, α = 103.100(7)°, β = 113.311(7)°, γ = 93.401(7)°, Z = 2]. As part of the unequivocal characterization of the aminooxyphosphenium salt, detailed solid-state ^{31}P NMR studies and GIAO calculations on the phosphenium cations have been performed. Contrary to popular belief, the phosphorus shielding in dicoordinate cations is not caused by the positive charge but results from efficient mixing between the phosphorus lone pair and π^* orbitals.

Introduction

Structural simplicity, high electrophilicity, and thermodynamic instability with respect to loss of N_2 are responsible for the diazonium cation **1** being one of the most fascinating and versatile classes of molecules.[2] In this light, isolation of a

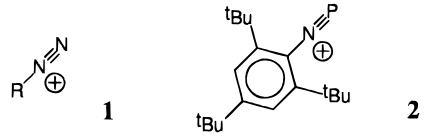

1

2

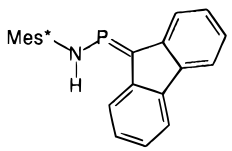

3

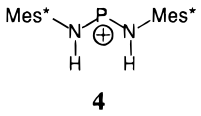

4

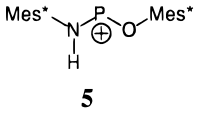

5

phosphadiazonium **2** (iminophosphenium)[3] salt and the gas-phase identification[4] of $[MeNP]^+$ represent landmarks in a systematic development of phosphorus chemistry. Limited studies into the reactivity of cation **2** include a novel cycloaddition reaction,[5] spectroscopic identification of a phosphine adduct,[6] and structural studies of arene adducts,[7,8] all of which implicate the Lewis acid or electrophilic nature of the phosphorus center.

Recognizing the potential synthetic utility and novel reactivity of **2**, our investigations have revealed a series of reactions which we describe here as nucleophilic additions. The reactions represent new syntheses for phosphaalkenes (**3**) and phosphenium cations (**4** and **5**), and all feature a facile and quantitative insertion of the N−P moiety into H−Y (Y = C, N, O) bonds. In addition, we present experimental support for a general reaction mechanism with the isolation and characterization of $[Mes^*NP{-}PPh_3][SO_3CF_3]$, (**6**)$[SO_3CF_3]$, a σ-complex model of a trapped intermediate for the insertion reaction.

Conclusive characterization of the new aminooxyphosphenium cation in **5**[$GaCl_4$] has been made possible by a solid-state ^{31}P NMR study. In addition, we have noted identical isotropic phosphorus chemical shifts for the phosphenium cation **4** and the neutral conjugate base Mes*N(H)PNMes*.[9] Therefore, we have carried out *ab initio* molecular orbital (MO) calculations of phosphorus chemical shieldings on model compounds using the gauge-including atomic orbitals (GIAO)

[⊗] Abstract published in *Advance ACS Abstracts,* August 15, 1996.

(1) On sabbatical leave from the Department of Chemistry, Mount Allison University, Sackville, New Brunswick.

(2) *The Chemistry of Diazonium and Diazo Groups*; Patai, S., Ed.; Wiley: New York, 1978.

(3) Niecke, E.; Nieger, M.; Reichert, F. *Angew. Chem., Int. Ed. Engl.* **1988**, *27*, 1715−1717. Niecke, E.; Nieger, M.; Reichert, F.; Schoeller, W. W. *Angew. Chem., Int. Ed. Engl.* **1988**, *27*, 1713−1715.

(4) Curtis, J. M.; Burford, N.; Parks, T. M. *Org. Mass Spectrom.* **1994**, *29*, 414−418.

(5) David, G.; Niecke, E.; Nieger, M. *Tetrahedron Lett*. **1992**, *33*, 2335−2338. David, G.; Niecke, E.; Nieger, M.; von der Gönna, V.; Schoeller, W. W. *Chem. Ber*. **1993**, *126*, 1513−1517.

(6) Niecke, E.; David, G.; Detsch, R.; Kramer, B.; Nieger, M.; Wenderoth, P. *Phosphorus, Sulfur Silicon Relat. Elem.* **1993**, *76*, 25−28.

(7) Gudat, D.; Schiffner, H. M.; Nieger, M.; Stalke, D.; Blake, A. J.; Grondey, H.; Niecke, E. *J. Am. Chem. Soc.* **1992**, *114*, 8857−8862.

(8) Burford, N.; Clyburne, J. A. C.; Bakshi, P. K.; Cameron, T. S. *J. Am. Chem. Soc.* **1993**, *115*, 8829−8830. Burford, N.; Clyburne, J. A. C.; Bakshi. P. K.; Cameron, T. S. *Organometallics* **1995**, *14*, 1578−1584.

(9) Gudat, D.; Hoffbauer, W.; Niecke, E.; Schoeller, W. W.; Fleischer, U.; Kutzelnigg, W. *J. Am. Chem. Soc.* **1994**, *116*, 7325−7331.

(10) (a) Wolinski, K.; Hinton, J. F.; Pulay, P. *J. Am. Chem. Soc.* **1990**, *112*, 8251−8260. (b) Pulay, P. *Theor. Chim. Acta* **1979**, *50*, 299−312.

S0020-1669(96)00131-0 CCC: $12.00

method.[10] The results of these studies enable us to present a detailed interpretation of phosphorus chemical shifts in these systems. Our results complement those of Niecke and coworkers.[9]

Experimental Section

General Procedures. Sample handling and reactions were performed under moisture free conditions.[11] Fluorene, *n*-butyllithium (1.6 M in hexanes), 2,4,6-tri-*tert*-butylaniline (Mes*NH_2), 2,4,6-tri-*tert*-butylphenol (Mes*OH), $AgSO_3CF_3$, and triphenylphosphine (Aldrich) were used as supplied. Mes*NPCl,[12] [Mes*NP][$GaCl_4$],[12] and [Mes*NP][SO_3CF_3][13] were prepared by literature methods. Dichloromethane was dried over CaH_2 and P_4O_{10}. Deuterated solvents were dried over CaH_2. Melting points were obtained on a Fisher-Johns apparatus and are uncorrected. FT-IR spectra, for the compounds as Nujol mulls on CsI plates, were recorded using a Nicolet 510P spectrometer. Chemical analyses were performed by Beller Laboratories, Göttingen, Germany. Solution $^{31}P\{^1H\}$, ^1H, and $^{13}C\{^1H\}$ NMR data were recorded at room temperature on samples sealed in evacuated Pyrex tubes using a Bruker AC-250 spectrometer (250.13 MHz for ^1H; 62.89 MHz for ^{13}C; 101.26 MHz for ^{31}P). Chemical shifts are reported in ppm relative to external standards (85% aqueous H_3PO_4 for ^{31}P; TMS for ^1H and ^{13}C). The salts exhibit low solubility in CD_2Cl_2, and therefore only peaks due to C−H substituted carbons are reported.

Preparation of Mes*N(H)P═Fluorenylidene (3) from Fluorenyllithium and Mes*NPCl. Fluorenyllithium (3.07 mmol, prepared *in situ* by the reaction of fluorene and BuLi) was added to a stirred solution (ether, 30 mL) of Mes*NPCl (3.14 mmol) at 0 °C. After 30 min, the volatiles were removed *in vacuo* and the solid was recrystallized from hexane to give orange crystals of **3**: isolated yield 39%; mp 207−209 °C dec. Anal. Calcd: C, 81.72; H, 8.41; N, 3.07. Found: C, 81.54; H, 8.50; N, 3.31. IR (cm^{-1}): 3413m, 1597m, 1308s, 1268s, 1217s, 1115s, 1026m, 1004m, 920s, 904s, 881s, 762s, 739s, 650m, 620m, 412m. NMR (CD_2Cl_2): $^{31}P\{^1H\}$, 256; ^1H, 7.92−7.79, 7.39−7.21 (aromatic 8H), 7.49 (s, 2H), 6.85 (d, J = 11 Hz, 1H), 1.34 (s, 18H), 1.36 (s, 9H); $^{13}C\{^1H\}$, 127.3 (d, J = 3 Hz), 126.8 (s), 126.6 (d, J = 5 Hz), 125.5 (d, J = 5 Hz), 123.8 (s), 123.2 (d, J = 4 Hz), 120.1 (s), 118.1 (d, J = 21 Hz), 33.48 (d, J = 3 Hz), 31.4 (s).

Preparation of [Mes*N(H)PN(H)Mes* (4)][$GaCl_4$] and [Mes*N(H)POMes* (5)][$GaCl_4$] from [Mes*NP (2)][$GaCl_4$]. In a typical procedure, a solution of Mes*NH_2 or Mes*OH (*ca*. 0.5 mmol in 20 mL of CH_2Cl_2) was added (10 min) to a stirred solution of a stoichiometric amount of [Mes*NP][$GaCl_4$] in *ca.* 20 mL of CH_2Cl_2.

Characterization Data for [Mes*N(H)PN(H)Mes* (4)][$GaCl_4$]: yellow block crystals recrystallized from CH_2Cl_2; yield 0.25 g, 0.32 mmol, 64%; mp 152−153.5 °C. Anal. Calcd: C, 56.94; H, 7.43; N, 3.69. Found: C, 56.79; H, 7.69; N, 3.57. IR (cm^{-1}): 3175s, 1599m, 1419m, 1396m, 1319m, 1271m, 1242m, 1212s 1178m, 1103s, 981s, 881s, 694m, 651w, 389s 376s, 362s. NMR (CD_2Cl_2): $^{31}P\{^1H\}$, 272; ^1H, 9.94 (d, 14 Hz, 2H), 7.54 (s, 4H), 1.57 (s, 36H), 1.32 (s, 18H); $^{13}C\{^1H\}$, 125.0 (s), 34.1 (s), 31.4 (s).

Characterization data for [Mes*N(H)POMes* (5)][$GaCl_4$]: yellow, sparingly soluble precipitate; yield 0.45 g, 98%; mp 160−163 °C. Anal. Calcd: C, 56.57; H, 7.78; N, 1.83. Found: C, 56.00; H, 7.75; N, 1.84. IR (cm^{-1}): 3120s, 1599m, 1418s, 1318m, 1305m, 1245m, 1219m, 1207s, 1165m, 1066s, 997s, 881s, 805s, 756m, 737m. 649w, 379s, 361s. NMR (CD_2Cl_2): $^{31}P\{^1H\}$, 296; ^1H, 10.9 (s, 1H), 7.59 (s, 2H), 7.48 (s, 2H), 1.60 (s, 18H), 1.58 (s, 18H), 1.40 (s, 9H); $^{13}C\{^1H\}$, 125.6 (s), 125.3 (s), 34.4 (s), 33.7 (s), 31.3 (s), 31.2 (s).

Preparation of [Mes*NP−PPh_3 (6)][SO_3CF_3]. [Mes*NP][SO_3CF_3] (0.21 g, 0.47 mmol) and PPh_3 (0.31 g, 0.47 mmol) were dissolved in hexanes (*ca.* 30 mL), and the mixture was stirred overnight, giving a small amount of creamy white solid with a clear orange solution, which were separated by decantation. Removal of solvent *in vacuo* gave orange-red crystals characterized as **6**[SO_3CF_3]: isolated yield 0.24 g, 0.34 mmol, 73%; mp 103−105 °C. Anal. Calcd: C, 63.33; H, 6.32; N, 2.00. Found: C, 63.92; H, 6.64; N, 2.11. IR (cm^{-1}): 1596m, 1583w(sh), 1493m, 1482m, 1362m, 1270w, 1260w, 1246w, 1231s, 1192vs, 1170s, 1102, 1030m, 991s, 883m, 831m(br), 761w, 745m, 691m, 632s, 578m, 494m, 442w, 352w, 268w. ^{31}P NMR data obtained for samples of redissolved crystalline **6**[SO_3CF_3]: −4, 56 (hexane); −5, 52 (toluene); −5, 52 (CD_2Cl_2). NMR spectra obtained on the same samples at 190 K are broadened with respect to the room-temperature spectra: −4, 56 (hexane); −7, 55 (toluene); 2, 79 broad (CD_2Cl_2). In all solution spectra, minor peaks are less than 1% (integrated) of the above peaks and there is no evidence for the two doublets consistent with **6**[SO_3CF_3] in the solvents used in the NMR solution studies.

Solution NMR Studies. Equimolar reaction mixtures were examined by ^{31}P NMR spectroscopy: **2**[$GaCl_4$] + Mes*NH_2, 272; **2**[$GaCl_4$] + Mes*OH, 296; Mes*NPCl + fluorenyllithium, 256; **2**[SO_3CF_3] + Mes*NH_2, 279; **2**[SO_3CF_3] + Mes*OH, 140.

Reaction of Mes*^{15}NPCl with Mes*N(H)Li. Equimolar quantities of Mes*NPCl (95% ^{15}N labeled) and LiN(H)Mes* were combined in ether at 0 °C. The solvent was removed *in vacuo* within 20 min and the solid was washed with hexanes. IR (cm^{-1}): 3344m (ν^{14}_{N-H}), 3337m (ν^{15}_{N-H}), 1599m, 1421s, 1303m, 1274s, 1241m, 1217m, 1114m, 888m, 879m, 768w, 523w. ^{31}P NMR (CD_2Cl_2): 269 (d, $^1J^{15}_{N-P}$ = 87 Hz), 269.8 (d, $^1J^{15}_{N-P}$ = 69 Hz).

Solid-State ^{31}P NMR Experiments. Solid-state ^{31}P NMR experiments were carried out using Bruker MSL-200 (B_0 = 4.7 T) and AMX-400 (B_0 = 9.4 T) spectrometers. Phosphorus-31 NMR spectra obtained with cross-polarization and magic-angle spinning (CP/MAS) were acquired using Bruker double-bearing MAS probes, with 3.5 μs proton pulse widths and recycle delays of 4−10 s. Chemical shifts were referenced with respect to external 85% aqueous H_3PO_4 by setting the peak of external solid [NH_4][H_2PO_4] to 0.8 ppm. The analysis of the spinning-sideband intensities in the MAS NMR spectra was carried out using a SIMPLEX least-squares routine based on extended Herzfeld−Berger ρ,μ tables.[14,15] The parameters obtained from the MAS spectra were refined using the first derivative of the absorption line shape of the static powder pattern. Calculations of the MAS and static powder patterns were performed using a 80486 microprocessor. The program WSolids, a program written in the C++ language and developed in our laboratory, was used for all calculations.

Quantum Mechanical Calculations. Molecular geometries of the model compounds were optimized by using Gaussian 92[16] and 6-311++G(D,P) basis sets and under preservation of the highest possible molecular symmetry. The GIAO calculations[10] were performed using a 6-311G basis set, augmented with two sets of polarization functions on all atoms. Absolute chemical shieldings were converted to chemical shifts using the absolute chemical shielding of 85% aqueous H_3PO_4, σ = 328.35 ppm.[17] All calculations were performed using an IBM RS6000/580 workstation. The drawing of the shape and symmetry of the MO's was generated using CACAO.[18]

X-ray Crystallography. Crystals were obtained as described above and mounted in Pyrex capillaries in a drybox. X-ray crystallographic data were collected on a Rigaku AFC5R diffractometer with graphite-monochromated MoK_α radiation (λ = 0.710 69 Å) for **3** and **4**[$GaCl_4$] and Cu Kα radiation (λ = 1.541 78 Å) for **6**[SO_3CF_3]. Unit cell parameters were obtained from the setting angles of a minimum of 20 carefully centered reflections having 2θ >20°; the choice of space groups was based on systematically absent reflections and confirmed by the successful solution and refinement of the structures.

Data were collected at room temperature (23 ± 1 °C) using the ω-2θ scan technique, and the stability of the crystals was monitored using three standard reflections. Data for **6**[SO_3CF_3] showed a 3.20% increase

(11) Burford, N.; Parks, T. M.; Müller, J. *J. Chem. Educ.* **1994**, *71*, 807−809.
(12) Burford, N.; Clyburne, J. A. C.; Losier, P.; Parks, T. M. In *Handbuch der Präparativen Anorganischen Chemie*, 4th ed. in English; Karsch, H. H., Ed.; Thieme-Verlag: Stuttgart, Germany, 1995.
(13) Niecke, E.; Detsch, R.; Nieger, M.; Reichert, F.; Schoeller, W. W. *Bull. Soc. Chim. Fr.* **1993**, *130*, 25−31.
(14) Herzfeld, J.; Berger, A. E. *J. Chem. Phys.* **1980**, *73*, 6021.
(15) (a) A. Kentgens, University of Nijmegen, The Netherlands. (b) Power, W. P.; Wasylishen, R. E. Unpublished results.
(16) Frisch, M. J.; Trucks, G. W.; Schlegel, H. B.; Gill, P. M. W.; Johnson, B. G.; Wong, M. W.; Foresman, J. B.; Robb, M. A.; Head-Gordon, M.; Replogle, E. S.; Gomperts, R.; Andres, J. L.; Raghavachari, K.; Binkley, J. S.; Gonzalez, C.; Martin, R. L.; Fox, D. J.; Defrees, D. J.; Baker, J.; Stewart, J. J. P.; Pople, J. A.; *Gaussian 92/DFT*, Revision F.2; Gaussian, Inc.: Pittsburgh, PA, 1993.
(17) Jameson, C. J.; De Dios, A.; Jameson, A. K. *Chem. Phys. Lett.* **1990**, *167*, 575−582.
(18) Mealli, C.; Proserpio, D. M. *J. Chem. Educ.* **1990**, *67*, 399−402.

Table 1. Crystallographic Data for **3**, **4**[$GaCl_4$], and **6**[SO_3CF_3][a]

	3	**4**[$GaCl_4$]	**6**[SO_3CF_3]
empirical formula	$C_{31}H_{38}NP$	$C_{36}H_{60}Cl_4GaN_2P$	$C_{37}H_{44}F_3NO_3P_2S$
fw	455.62	763.39	701.76
T (°C)	23	23	23
radiation	Mo Kα	Mo Kα	Cu Kα
space group	$P2_1/c$ (No. 14)	$C2/c$ (No. 15)	$P\bar{1}$ (No. 2)
a (Å)	9.568(8)	24.921(2)	10.663(1)
b (Å)	24.25(2)	10.198(4)	19.439(1)
c (Å)	11.77(1)	16.445(2)	10.502(1)
α (deg)			103.100(7)
β (deg)	101.38(8)	93.32(1)	113.311(7)
γ (deg)			93.401(7)
V (Å^3)	2678(3)	4172(1)	1920(1)
Z	4	4	2
ρ_{calcd} (g cm^{-3})	1.130	1.215	1.214
μ (cm^{-1})	1.209	9.785	19.453
goodness-of-fit	1.533	1.083	1.937
R; R_w	0.0607; 0.0649	0.0344; 0.0369	0.0464; 0.0475

[a] $R = \sum(|F_o| - |F_c|)/\sum|F_o|$. $R_w = \{\sum[w(|F_o| - |F_c|)^2]/\sum w|F_o|^2\}^{1/2}$. Goodness-of-fit $= \sum(|F_o| - |F_c|)/(n - m)$; n = number of reflections used in refinement; m = number of variables.

in intensity of the standards during data collection; a linear correction factor was applied. The other compounds showed no changes in intensity. Data were corrected for Lorentz and polarization effects. An empirical absorption correction, based on azimuthal scans of several reflections, was applied to **6**[SO_3CF_3]. The data for **6**[SO_3CF_3] and **4**[$GaCl_4$] were also corrected for secondary extinction.

Structures were solved by direct methods[19] and expanded using successive Fourier syntheses. All non-hydrogen atoms were refined anisotropically. All of the hydrogen atoms were placed in geometrically calculated positions with C−H distances of 1.08 Å and N−H distances of 1.02 Å. Their positions were not refined, and they were assigned fixed isotropic temperature factors with a value of $1.2B_{eq}$ of the atom to which it was bonded. The function minimized by full-matrix least squares was $\sum w(F_o - F_c)^2$ (unit weights). Neutral-atom scattering factors were taken from Cromer and Waber.[20] Anomalous dispersion effects were included in F_c;[21] the values for $\Delta f'$ and $\Delta f''$ were those of Creagh and McAuley.[22] The values for the mass attenuation coefficients were those of Creagh and Hubbell.[23] All calculations were performed using the teXsan crystallographic software package of Molecular Structure Corp.[24] Crystallographic details are summarized in Table 1.

The location of the hydrogen atom on the C−N−P fragment of **3** was not determined. A difference map at the final stages of refinement indicated a peak at 0.5374, 0.6344, 0.6320 (height 0.8). If a hydrogen is placed geometrically on N(1) (1.02 Å, 120°), the height of this peak after refinement diminishes but not significantly (height 0.63). This is because the peak is not located where it would normally be expected. A difference map illustrating this difficulty has been deposited with the Supporting Information. This hydrogen atom was not included in the final solution; however, evidence for the N−H bond is provided by IR data. It is possible that the hydrogen atom position is influenced by intramolecular hydrogen bonding to the fluorenylidene substituent; no evidence for intramolecular hydrogen bonding was observed. The least-squares plane defined by P(1), N(1), fluorenylidene [C(1)−C(13)], and C(14) of Mes* has a mean deviation of 0.017 Å.

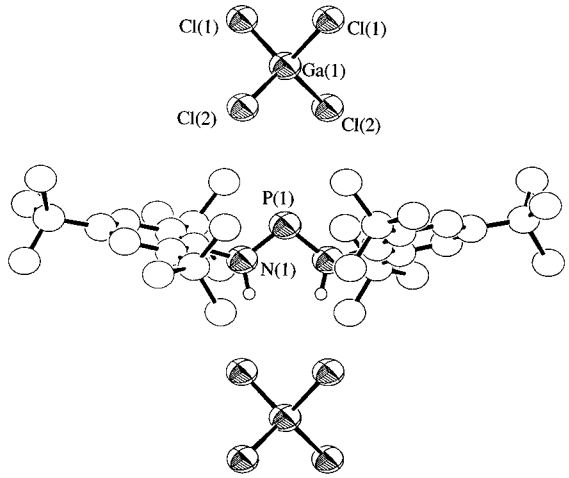

Figure 1. Partial ORTEP view of **4**[$GaCl_4$]. The hydrogen atoms (except N−H) have been omitted for clarity.

Table 2. Selected Bond Lengths (Å) and Angles (deg) for **4**[$GaCl_4$] and Comparative Parameters for Mes*N(H)PNMes* [29]

[Mes*N(H)PN(H)Mes*][$GaCl_4$]		Mes*N(H)PNMes*	
Ga(1)−Cl(1)	2.188(1)		
Ga(1)−Cl(2)	2.153(2)		
P(1)−N(1)	1.617(3)	P(1)−N(1)	1.573(8)
		P(1)−N(2)	1.633(8)
N(1)−C(1)	1.471(5)		
P(1)- - -Cl(2)	3.853(2)		
Cl(1)- - -N(1)	3.405(4)		
Cl(1)−Ga(1)−Cl(1)	104.72(8)		
Cl(1)−Ga(1)−Cl(2)	109.33(6)		
Cl(1)−Ga(1)−Cl(2)	110.41(7)		
N(1)−P(1)−N(1)	103.9(2)	N(1)−P(1)−N(1)	103.8(5)
P(1)−N(1)−C(1)	126.3(3)	P(1)−N(1)−C(1)	126.1(7)
		P(1)−N(1)−C(2)	126.5(7)
N(1)−C(1)−C(2)	120.3(3)		
N(1)−C(1)−C(6)	117.5(3)		

Results and Discussion

Reactions of the Phosphadiazonium Cation with Fluorenylide, Mes*NH_2, and Mes*OH. The Lewis acid and/or electrophilic nature of **2** is apparent from the extreme moisture sensitivity of the $[AlCl_4]^-$, $[GaCl_4]^-$, and $[Ga_2Cl_7]^-$ salts, as well as the observation of phosphine[3] and arene[8] donor/acceptor complexes of the cation, where the sterically imposing Mes* (2,4,6-tri-*tert*-butylphenyl) substituent seems to aid in isolation of reaction products. In this study, we have observed (^{31}P NMR of reaction mixtures sealed under vacuum) rapid and quantitative reactions of **2**[$GaCl_4$] with Mes*NH_2 and Mes*OH in CH_2Cl_2 at room temperature. The products were characterized as tetrachlorogallate salts of the diaminophosphenium cation **4** and the new aminooxyphosphenium cation **5**, respectively. The solid-state structure of **4**[$GaCl_4$] was confirmed by X-ray crystallography (Figure 1) and is essentially identical to that of the recently reported $[AlCl_4]^-$ salt.[25] Bond lengths and angles for the cation (Table 2) are also consistent with the established data for diaminophosphenium salts,[26,27] including [Mes*N(H)-PN(*i*-Pr)$_2$][SO_3CF_3].[28] Notable is the hydrogen bonding between anion and cation, and a one-dimensional polymeric lattice

(19) Sheldrick, G. M. SHELXS-86. In *Crystallographic Computing 3*; Sheldrick, G. M., Krüger, C., Goddard, R., Eds.; Oxford University Press: Oxford, U.K., 1985; pp 175−189.
(20) Cromer, D. T.; Waber, J. T. *International Tables for X-ray Crystallography*; Kynoch Press: Birmingham, England, 1974; Vol. IV, Table 2.2A.
(21) Ibers, J. A.; Hamilton, W. C. *Acta Crystallogr.* **1964**, *17*, 781−782.
(22) Creagh, D. C.; McAuley, W. J. In *International Tables for X-ray Crystallography*; Wilson, A. J. C., Ed.; Kluwer Academic Publishers: Boston, 1992; Vol. C, Table 4.2.6.8, pp 219−222.
(23) Creagh, D. C.; Hubbell, J. H. In *International Tables for X-ray Crystallography*; Wilson, A. J. C., Ed.; Kluwer Academic Publishers: Boston, 1992; Vol. C, Table 4.2.4.3, pp 200−206.
(24) *teXsan−Crystal Structure Analysis Package*; Molecular Structure Corp.: The Woodlands, TX, 1985 and 1992.
(25) Nieger, M.; Niecke, E.; Detsch, R. *Z. Kristallogr.* **1995**, *210*, 971−972.
(26) See, for example: Sanchez, M.; Mazieres, M. R.; Lamande, L.; Wolf, R. In *Multiple Bonds and Low Coordination in Phosphorus Chemistry*; Regitz, M., Scherer, O. J., Eds.; Georg Thieme Verlag: Stuttgart, Germany, 1990; pp 129−148. Cowley, A. H.; Kemp, R. A. *Chem. Rev.* **1985**, *85*, 367−382
(27) Burford, N.; Losier, P.; Macdonald, C.; Kyrimis, V.; Bakshi, P. K.; Cameron, T. S. *Inorg. Chem.* **1994**, *33*, 1434−1439.
(28) Drapailo, A. B.; Chernega, A. N.; Romanenko, V. D.; Madhouni, R.; Sotiropoulos, J.-M.; Lamande, L.; Sanchez, M. *J. Chem. Soc., Dalton Trans.* **1994**, 2925−2931.

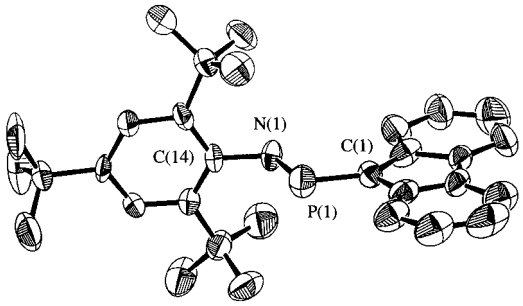

Figure 2. ORTEP view of **3**. The hydrogen atoms have been omitted for clarity.

Table 3. Selected Bond Lengths (Å) and Angles (deg) for **3**

		Lengths	
P(1)−N(1)	1.655(8)	N(1)−C(14)	1.45(1)
P(1)−C(1)	1.707(9)		
		Angles	
N(1)−P(1)−C(1)	109.3(5)	P(1)−C(1)−C(13)	116.9(8)
P(1)−N(1)−C(14)	119.7(6)	C(2)−C(1)−C(13)	106.9(9)
P(1)−C(1)−C(2)	136.2(8)		

resulting from interionic contacts between the phosphorus center and a second anion, which imposes a tetracoordinate environment on the phosphorus center. These contacts distort the anion but have no obvious effect on the structural parameters of the cation (in comparison to related diaminophosphenium cations). It is interesting to note that the structural features of **4** are very similar to those of its conjugate base Mes*N(H)PNMes* (compared in Table 2).[29]

Although it was not possible to obtain a crystalline sample of **5**[$GaCl_4$] suitable for crystallographic study, chemical analysis, solution NMR spectra, and the distinct N−H band in the infrared spectrum are consistent with a phosphenium salt and are comparable with the data for **4**[$GaCl_4$]. In addition, we have performed a thorough solid-state ^{31}P NMR study of both salts, and our theoretical modeling provides convincing support for the structural assignment (*vide infra*).

Our observations for the reaction of Mes*NPCl with fluorenyllithium in diethyl ether are related to the results above. The new phosphaalkene derivative **3** is formed quantitatively (as shown by ^{31}P NMR of the reaction mixture), and the secondary amine at the former imine site is once again confirmed by the infrared band at 3413 cm^{-1}. Moreover, a crystallographic study reveals the characteristic features for aminophosphaalkenes,[30] as illustrated in Figure 2. Selected bond lengths and angles are presented in Table 3.

Mechanism of Nucleophilic Addition to the Phosphadiazonium Cation. The formation of compounds **3**, **4**[$GaCl_4$], and **5**[$GaCl_4$] can be classified in terms of a formal insertion of the Mes*NP moiety into the H−Y bond (Y = C, N, O), demonstrating a general reaction for the phosphadiazonium cation. More importantly, the reactions represent quantitative processes for the synthesis of phosphaalkenes and phosphenium cations, including the first oxy derivative **5**. On the basis of the acceptor potential for the phosphorus center in **2** and the electron-rich (donor) nature of the three reagents under investigation, we envisage the reactions to proceed *via* a coordination complex intermediate.

The reaction of Mes*NPCl with fluorenyllithium is considered as a metathesis giving [Mes*NP][fluorenylide], which then offers the potential for P−C bond formation and only requires a 1,3-H migration to generate the observed product **3**. This is consistent with previous observations for alkyl-substituted iminophosphines which rearrange to aminophosphaalkenes by a 1,3-shift of an α-hydrogen atom or silyl group.[31] In this context, the crystal structure of Mes*NP−Cp* (**8**) is viewed as an $^1\eta$ complex of **2** with [Cp*$^-$][7] and as a model for the proposed intermediate **7**; however, the 1,3-methyl migration from Cp* in **8** has not been observed.

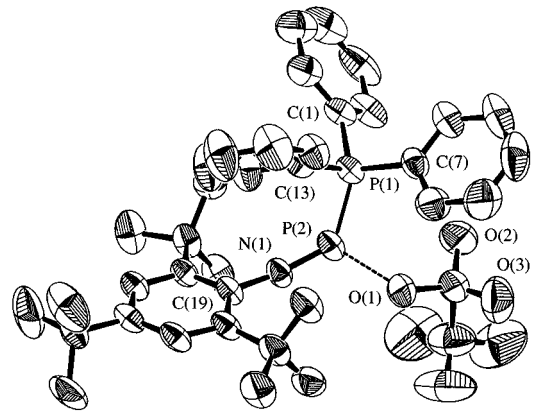

Figure 3. ORTEP view of **6**[SO_3CF_3]. Hydrogen atoms have been omitted for clarity.

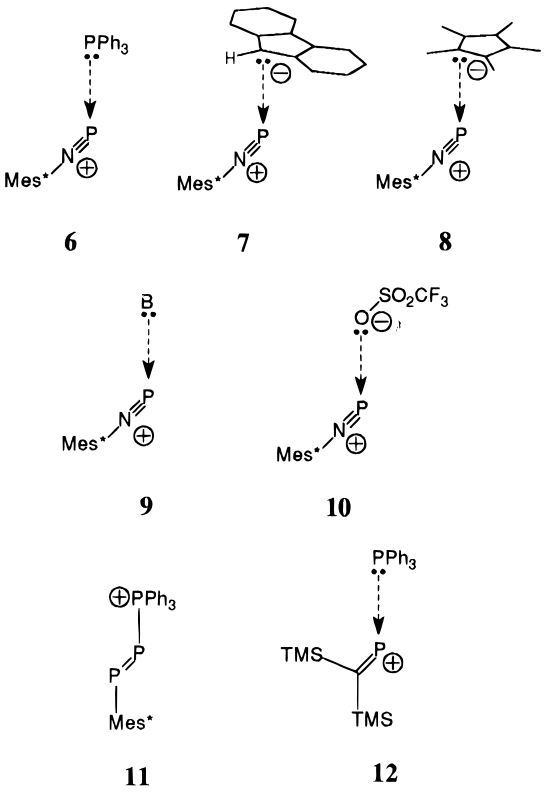

An analogous process is proposed for the formation of **4** and **5**. However, examples for σ complexes (**9**) of **2** have not yet been structurally characterized, the closest model being Mes*NPI.[31] The reaction of **2**[$AlCl_4$] with PPh_3 was postulated to form the cationic complex [Mes*NP−PPh_3]$^+$ (**6**) (on the basis of solution ^{31}P NMR spectroscopy),[6] and the rearrangement of this cation to the phosphenium alternative is probably avoided by the absence of a Y−H bond (Y = P for **6**). We have now isolated the triflate salt of **6**, and the crystal structure is shown in Figure 3. Selected bond lengths and angles are compared in

(29) Hitchcock, P. B.; Lappert, M. F.; Rai, A. K.; Williams, H. D. *J. Chem. Soc., Chem. Commun.* **1986**, 1633−1634.

(30) Appel, R. In *Multiple Bonds and Low Coordination in Phosphorus Chemistry*; Regitz, M., Scherer, O. J., Eds.; Georg Thieme Verlag: Stuttgart, Germany, 1990; pp 157−219.

(31) Niecke, E.; Gudat, D. *Angew. Chem., Int. Ed. Engl.* **1991**, *30*, 217−237.

Table 4. Selected Bond Lengths (Å) and Angles (deg) for **6**[SO_3CF_3] and a Comparison with Parameters for **10**[13]

[Mes*NP−PPh_3][SO_3CF_3]		[Mes*NP][SO_3CF_3]	
S(1)−O(1)	1.467(4)	S(1)−O(1)	1.499(4)
S(1)−O(2)	1.428(4)	S(1)−O(2)	1.405(4)
S(1)−O(3)	1.427(5)	S(1)−O(3)	1.409(5)
P(1)−C(1)	1.814(6)		
P(1)−C(7)	1.811(5)		
P(1)−C(13)	1.812(6)		
P(2)−N(1)	1.486(4)	P(1)−N(1)	1.467(4)
P(2)−O(1)	2.298(4)	P(1)−O(1)	1.923(3)
P(1)−P(2)	2.625(2)		
N(1)−C(19)	1.404(6)		
C(1)−P(1)−P(2)	98.1(2)		
C(7)−P(1)−P(2)	121.6(2)		
C(13)−P(1)−P(2)	114.9(2)		
C(1)−P(1)−C(7)	107.8(3)		
C(1)−P(1)−C(13)	105.4(3)		
C(7)−P(1)−C(13)	107.2(2)		
P(2)−N(1)−C(19)	169.5(4)	P(1)−N(1)−C(1)	176.4(3)
O(1)−P(2)−N(1)	111.1(2)	O(1)−P(1)−N(1)	108.4(2)
P(1)−P(2)−N(1)	109.8(2)		

Table 4 with those of previously reported [Mes*NP][SO_3CF_3] (**10**).[13] The shortest anion---cation interaction in **6**[SO_3CF_3] [P(2)---O(1) 2.298(4) Å] is significantly longer than that observed for **10** [P---O 1.923(3) Å]. Moreover, the unique S−O bond (*i.e.*, S−O---P) in **6**[SO_3CF_3] is significantly shorter than the corresponding S−O bond in **10**, and the two remaining S−O bonds are slightly longer, implying more ionic character for the $[SO_3CF_3]^-$ ion in **6**[SO_3CF_3]. Therefore, the interaction of PPh_3 competes with the donor−acceptor interaction of the anion (*i.e.*, S−O→P) effecting displacement of $[SO_3CF_3]^-$ relative to **10**.

The new cationic complex $[Mes*NP-PPh_3]^+$ (**6**) exhibits some interesting structural features, including an unusually long P−P bond [2.625(2) Å]. The nearly linear geometry at nitrogen [169.5(4)°] and the short NP bond [1.486(4)Å] are similar to many structures containing the Mes*NP moiety, including Mes*NPCl [NP 1.475(8)Å, CNP 177.0(7)°],[3] Mes*NPI [NP 1.480(3)Å, CNP 172.5(3)°],[31] [Mes*NP][SO_3CF_3] [NP 1.467(4)Å, CNP 176.4(3)°][13] and [Mes*NP−benzene][Ga_2Cl_7] [NP 1.463-(5)Å, CNP 178.5(4)°],[8] which demonstrate weak interaction with the anion or ligand and retention of NP triple-bond character. In contrast, Mes*NPCp* [NP 1.551(8)Å, CNP 125.9(6)°][7] is best viewed as a covalent iminophosphine structural alternative to the anion-cation complex **8** due to an effective σ interaction between the formerly more basic anionic carbon and the cationic phosphorus. We find it interesting that the 3-fold axis of the PPh_3 ligand in **6**[SO_3CF_3] is directed away from the phosphorus center of $[Mes*NP]^+$ [C(1)−P(1)−P(2) 98.1(2)°, C(7)−P(1)−P(2) 121.6(2)°, C(13)−P(1)−P(2) 114.9(2)°].

The recently reported structures of [Mes*P═P−PPh_3 (**11**)]-[BPh_4][32] and [$(SiMe_3)_2$C═P−PPh_3 (**12**)][$AlCl_4$][33] offer useful comparisons. The P−PPh_3 bond [2.206(1)Å] in cation **11** is typical of (or slightly shorter than) a single bond (2.22 Å),[34] and the small C_{ipso}PP bond angle at Mes*PP [98.8(2)°] highlights the molecule as a diphosphene−phosphonium cation consistent with spectroscopic and theoretical evaluations.[32] A slightly longer P−P bond [2.267(2) Å] is observed for cation **12**, and the molecule has been described in terms of a partial coordinative interaction, recognizing the formal electron deficiency at the phosphorus site. As observed for cation **6**, the 3-fold axis of the PPh_3 ligand of cation **12** is displaced from the P−P vector, albeit to a lesser degree [C(20)−P(2)−P(1) 112°, C(14)−P(2)−P(1) 101°, C(8)−P(2)−P(1) 116°].[33]

The dramatically longer P−P bond observed for **6** as well as the relatively unperturbed structure of the Mes*NP moiety implies that this coordinative interaction is weaker than in both **11** and **12**. This is perhaps due to the competitive donation from the triflate anion but more importantly is a function of the resilience of the triple-bond character of the NP bond[35] in the phosphadiazonium cation. In comparison, the triple bond of the diphosphadiazonium ($Mes*PP^+$) acceptor would be substantially weaker than the NP multiple bond in $Mes*NP^+$ and therefore more susceptible to disruption by the approach of the ligand. Hence, the molecule adopts the P═P double-bonded diphosphene−phosphonium **11** electronic structure. The orbital vacancy at phosphorus in the methylenephosphenium cation ($(TMS)_2C{=}P^+$) allows for a full coordinative bond in **12**, without coordinative competition.

1,3-Hydrogen migrations,[36] as well as the related methyl[37] and trimethylsilyl migrations,[6,38] have been documented for neutral iminophosphines as well as a metalloiminophosphine[39] but are usually facilitated by an external base or by heating, except in the case of Mes*N(H)PNMes*.[29] The facile nature of the 1,3-hydrogen migration for Mes*N(H)PNMes* is confirmed by a ^{15}N-labeling study. Mes*^{15}NPCl reacts with LiN(H)Mes* in ether (0 °C), and isolation of the reaction product after only 20 min in solution indicates a 1:1 mixture of two isotopomers, Mes*N(H)P^{15}NMes* and Mes*NP^{15}N(H)Mes*, as determined by IR and ^{31}P NMR spectroscopy. Prototropic equilibria are well-established for triazenes.[40] In addition, the reaction of a diazonium cation with primary and secondary amines to give triazenes likely involves a similar process and an intermediate nitrenium cation; but these reactions are typically performed in the presence of a suitable base which deprotonates any charged intermediates.[2]

Solid-State ^{31}P NMR of Dicoordinate Phosphorus Centers. Confirmation of the structural assignment for **5**[$GaCl_4$] required a comparative study of ^{31}P NMR spectra in the solid state. This study also provides information about the phosphorus chemical shift tensors. As will be shown below, this information is crucial in providing an interpretation of phosphorus chemical shifts in these systems.

Phosphorus-31 NMR spectra of solid powder samples of **4**[$GaCl_4$] and **5**[$GaCl_4$] were obtained under conditions of magic-angle spinning (MAS) and also for stationary samples. The ^{31}P MAS NMR spectra provide isotropic chemical shifts and information about the number of crystallographically distinct molecules in the asymmetric unit. Spectra of stationary powder samples enable one to characterize the phosphorus chemical shift tensors for these systems. When phosphorus is adjacent to a magnetically active nucleus (*e.g.* ^{14}N or ^{31}P), spin−spin coupling data can be obtained from spectra obtained with or without MAS. The isotropic chemical shifts and principal components of the chemical shift tensors are summarized in Table 5.

(32) Romanenko, V. D.; Rudzevich, V. L.; Rusanov, E. B.; Chernega, A. N.; Senio, A.; Sotiropoulos, J.-M.; Pfister-Guillouzo, G.; Sanchez, M. *J. Chem. Soc., Chem. Commun.* **1995**, 1383−1385.
(33) David, G.; Niecke, E.; Nieger, M.; Radseck, J. *J. Am. Chem. Soc.* **1994**, *116*, 2191−2192.
(34) Corbridge, D. E. C. *Phosphorus: An Outline of its Chemistry, Biochemistry and Technology*, 4th ed.; Elsevier: Amsterdam, 1990.
(35) Curtis, R. D.; Schriver, M. J.; Wasylishen, R. E. *J. Am. Chem. Soc.* **1991**, *113*, 1493−1498.
(36) Niecke, E.; Altmeyer, O.; Barton, D.; Detsch, R.; Gartner, C.; Hein, J.; Nieger, M.; Reichert, F. *Phosphorus, Sulfur Silicon Relat. Elem.* **1990**, *49/50*, 321−324. Niecke, E.; Gudat, D. *Angew. Chem., Int. Ed. Engl.* **1991**, *30*, 217−342.
(37) Burford, N.; Mason, S.; Spence, R. E. v. H.; Whalen, J. M.; Richardson, J. F.; Roders, R. D. *Organometallics* **1992**, *11*, 2241−2250.
(38) Zurmühlen, F.; Regitz, M. *Angew. Chem., Int. Ed. Engl.* **1987**, *26*, 83−84.
(39) Niecke, E.; Hein, J.; Nieger, M. *Organometallics* **1989**, *8*, 2290−2292.
(40) See, for example: Hooper, D. L.; Vaughan, K. *J. Chem. Soc., Perkin Trans. 2* **1981**, 1161−1165.

Table 5. Experimental and Calculated[a] Phosphorus Chemical Shift Tensors (in ppm) of Phosphaalkyne, Phosphadiazonium, Aminophosphenium, and Iminophosphine Centers (R = Mes*)

	δ_{iso}	δ_{11}	δ_{22}	δ_{33}	Ω[b]	κ[c]	α[d] (deg)
R−C≡P[e]	31	229	140	−274	503	0.65	
[R−N≡P][$AlCl_4$][f]	77	308	196	−273	581	0.61	
[R−N≡P*−PPh_3 (**6**)][SO_3CF_3]	71[g,h]	307	174	−269	576	0.54	
[R−N≡P−P*Ph_3 (**6**)][SO_3CF_3]	−1[g]	15	0	−18	33	0.03	
RNH−P═NR[i]	281	628	124	90	538	−0.87	
[RNH−P−NHR (**4**)][$GaCl_4$]	281[j]	624	167	51	573	−0.59	
[RNH−P−OR (**5**)][$GaCl_4$]	306, 303[k]	670	124	124	546	−1.00	
H_2N−P═NH	301	815	58	31	784	−0.93	7
[H_2N−P−NH_2]$^+$	242	623	136	−32	655	−0.49	38
[H_2N−P−OH]$^+$	268	692	59	54	638	−0.98	48

[a] Calculated chemical shieldings have been converted to chemical shifts using $\delta = 328$ ppm $- \sigma$.[17] [b] Span of chemical shift tensor, $\Omega = \delta_{11} - \delta_{33}$. [c] Skew of chemical shift tensor, $\kappa = 3(\delta_{22} - \delta_{iso})/\Omega$. [d] Angle between δ_{11} and the H_2N−P bond, measured toward the phosphorus lone pair; the direction of highest shielding is perpendicular to the molecular plane. [e] Reference 51. [f] Reference 35. [g] $^1J(^{31}P,^{31}P) = -405(5)$ Hz. [h] $|^1J(^{31}P,^{14}N)| < 20(5)$ Hz. [i] Reference 9. [j] $|^1J(^{31}P,^{14}N)| = 60$ Hz. [k] Two crystallographically nonequivalent molecules in a 2:1 ratio with indistinguishable chemical shift tensors.

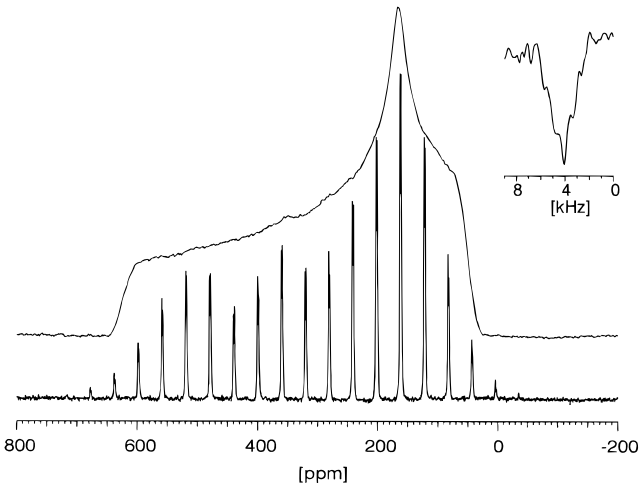

Figure 4. Solid-state ^{31}P NMR spectra of **4**[$GaCl_4$] obtained at 4.7 T. The bottom trace shows the MAS spectrum for a sample spinning at 3.2 kHz, with 112 scans. The upper trace shows the spectrum of a stationary sample with 25 600 scans. The upper right insert shows an expansion of the first derivative of the low-frequency region of the static pattern, illustrating the effect of $^{31}P-^{14}N$ dipolar interactions; the splittings are 800 Hz.

The ^{31}P NMR spectra obtained for a solid sample of **4**[$GaCl_4$] are shown in Figure 4. The isotropic region of the ^{31}P CP/MAS NMR spectrum consists of a multiplet of three equally spaced peaks with an intensity ratio of 4:4:1. This pattern arises from the combined residual direct dipolar and indirect spin−spin interactions of ^{31}P with two quadrupolar ^{14}N nuclei.[41] Analysis of this pattern reveals $|^1J(^{31}P,^{14}N)| = 60(5)$ Hz, which is in good agreement with the value determined from a sample partially enriched in ^{15}N and dissolved in dichloromethane, $^1J(^{31}P,^{15}N) = 87$ Hz, given that $\gamma(^{15}N)/\gamma(^{14}N) = -1.403$. The residual dipolar coupling[41] is −22 Hz at 4.7 T, which is comparable to −25 Hz calculated from reasonable estimates of this parameter ($\nu_{^{14}N} = 14.44$ MHz, $R = 800$ Hz, $\beta = 90°$, $\chi(^{14}N) = -3$ MHz, $\eta = 0$). The ^{31}P NMR line shape of the stationary powder sample does not provide any obvious evidence for $^{31}P,^{14}N$ direct dipolar interactions. However, the first derivative of the line shape in the δ_{33} region exhibits equally spaced splittings of *ca.* 800 Hz, which corresponds to the value of the direct dipolar coupling constant calculated from the known P−N bond separation ($r_{PN} = 1.613$ Å). This observation suggests that δ_{33} is oriented perpendicular to the plane containing the two P−N bonds,[42] which is confirmed by the *ab initio* MO calculations on $H_2N-P-NH_2^+$ (*vide infra*).

The ^{31}P CP/MAS NMR spectra of **5**[$GaCl_4$] at 4.7 and 9.4 T indicate the presence of two crystallographically distinct molecules in the ratio 2:1 with isotropic chemical shifts of 306 and 303 ppm, respectively. Spin−spin interactions involving ^{14}N were not resolved in this case. The principal components of the chemical shift tensor determined from the line shape of the stationary powder sample indicate that the tensor is axially symmetric within experimental error. Compared to the related **4**[$GaCl_4$], the phosphorus nucleus is less shielded in **5** by about 20 ppm, primarily due to a change in δ_{11}; also, while δ_{22} and δ_{33} have similar values for **5**, they are quite different for **4**.

Phosphorus-31 MAS NMR spectra of solid samples of [Mes*NP−PPh_3 (**6**)][SO_3CF_3] indicate two phosphorus centers with isotropic chemical shifts characteristic of the [MesNP]$^+$ and triphenylphosphine moieties. Spectra of stationary samples confirm that the phosphorus chemical shift tensor of the Mes*NP fragment is only marginally perturbed by coordination of the PPh_3 ligand. Compared to the phosphorus chemical shift tensor of solid PPh_3, $\delta_{11} = \delta_{22} = 9$, $\delta_{33} = -42$ ppm,[43] the apparent axial symmetry about phosphorus of PPh_3 is clearly perturbed in **6**, consistent with the structural data (*vide supra*). Interestingly, the two phosphorus nuclei are strongly coupled to one another, $^1J(^{31}P,^{31}P) = -405$ Hz. Thus, in spite of the unusually long P−P bond in this adduct, it appears that substantial orbital overlap at these two centers must exist to be compatible with such a large J coupling. The sign of $^1J(^{31}P,^{31}P)$ was determined from the splittings observed along the F_1 domain of the 2D spin-echo spectrum.[44] A complete discussion of $J(^{31}P,^{31}P)$ in this and related systems is beyond the scope of the present paper.

***Ab Initio* Molecular Orbital Calculations on Aminophosphenium Moieties.** Traditionally, the very deshielded ^{31}P nuclei at phosphenium centers have been rationalized in terms of the positive charge located at phosphorus.[26,45] A comparison of the phosphorus chemical shift tensors of the phosphenium compounds presented in this study with those of similar neutral

(41) (a) Harris, R. K.; Olivieri, A. C. *Prog. NMR Spectrosc.* **1992**, *24*, 435−456. (b) Eichele, K.; Wasylishen, R. E. *Inorg. Chem.* **1994**, *33*, 2766−2773.

(42) (a) Eichele, K.; Wasylishen, R. E. *J. Magn. Reson. A* **1994**, *106*, 46−56. (b) Wasylishen, R. E.; Curtis, R. D.; Eichele, K.; Lumsden, M. D.; Penner, G. H.; Power, W. P.; Wu, G. In *Nuclear Magnetic Shieldings and Molecular Structure*; Tossell, J. A., Ed.; NATO ASI Series Vol. 386; Kluwer Academic Publishers: Dordrecht, The Netherlands, 1993, pp 297−314.

(43) Penner, G. H.; Wasylishen, R. E. *Can. J. Chem.* **1989**, *67*, 1909−1913.

(44) Eichele, K.; Wasylishen, R. E.; Schurko, R. W.; Burford, N.; Whitla, W. A. *Can. J. Chem.*, in press.

(45) (a) Fluck, E.; Heckmann, G. In *Phosphorus-31 NMR Spectroscopy in Stereochemical Analysis*; Verkade, J. G., Quin, L. D., Eds.; VCH Publishers: Deerfield Beach, FL, 1987; pp 61−113. (b) Zhang, C.-J.; Zhan, C.-G.; Huang, T.-B. *J. Mol. Struct.* **1995**, *357*, 9−18.

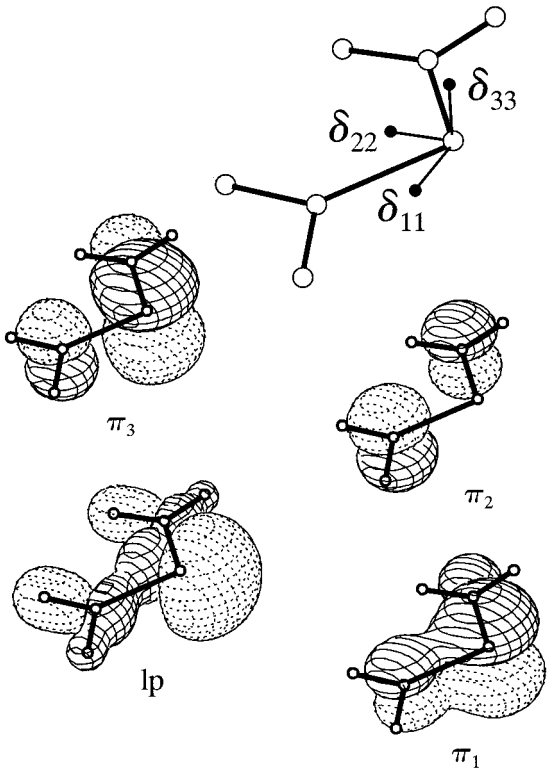

Figure 5. Orientation of the phosphorus chemical shift tensor in $[H_2N-P-NH_2]^+$ as obtained from *ab initio* calculations: the most shielded direction is perpendicular to the molecular plane, the direction of intermediate shielding bisects the NPN angle, and the direction of least shielding is within the molecular plane and perpendicular to the supposed lone pair of electrons at phosphorus. On the bottom, the shape of the frontier MO's is depicted, where π_1, lp, and π_2 are filled (π_2 is the HOMO) and π_3 is the LUMO. The mixing responsible for the deshielding along δ_{11} occurs between lp and π_3.

parent compounds, thoroughly investigated by Gudat *et al.*,[9] clearly demonstrates that this interpretation required re-evaluation. For example, the phosphorus isotropic chemical shift of Mes*N(H)−P═NMes* has been reported as 281 ppm,[9] which is identical to the chemical shift found for the cation **4**. As a comparison of the principal components of the phosphorus chemical shift tensors of both compounds reveals, the structural change does not affect δ_{11} but shifts δ_{22} and δ_{33} in such a manner that the average value, δ_{iso}, remains the same. In order to gain a better insight into the cause of the deshielding observed for the cations, we carried out *ab initio* GIAO[10] quantum mechanical calculations of phosphorus chemical shieldings for simple model compounds, *viz.*, $H_2N-P═NH$, $[H_2N-P-NH_2]^+$, and $[H_2N-P-OH]^+$. The calculated principal components and the orientations of the phosphorus chemical shielding tensors of these compounds, converted to chemical shifts, are included in Table 5.

Generally, *ab initio* calculations of chemical shieldings yield very reliable information regarding the orientation of the chemical shielding tensor in the molecular frame of reference. In Figure 5, we show the orientation of the phosphorus chemical shift tensor calculated for $[H_2N-P-NH_2]^+$. The direction of highest shielding, *i.e.*, the direction associated with δ_{33}, is perpendicular to the molecular plane, while the direction of intermediate shielding lies approximately along the direction of the formal lone pair of electrons at phosphorus. The direction of least shielding is found perpendicular to the lone pair and within the molecular plane. Analogous results are obtained for $H_2N-P═NH$ and $[H_2N-P-OH]^+$.

The trends in the changes of the chemical shift tensors on going from $H_2N-P═NH$ to $[H_2N-P-NH_2]^+$ and $[H_2N-P-OH]^+$ compare well with experimental values. In contrast to the expectations based on charge arguments,[26] the calculations predict that the phosphorus in the neutral $H_2N-P═NH$ should be even less shielded than in $[H_2N-P-NH_2]^+$. For $H_2N-P═NH$, the GIAO calculations appear to overestimate the deshielding along the direction of δ_{11}. This deficiency in theoretical methods is also apparent from IGLO calculations on related neutral compounds.[9] Generally, calculations of chemical shieldings at the Hartree−Fock level involving species with low-lying virtual states tend to overestimate the paramagnetic contribution due to neglect of electron correlation, and this is aggravated by the presence of diffuse lone pairs at the nucleus under consideration. It is interesting to note the trends observed and calculated for δ_{22} and δ_{33}. In the neutral parent compound, the difference between δ_{22} and δ_{33} is only 30 ppm, but it increases substantially in the cation, while for $[H_2N-P-OH]^+$ δ_{22} and δ_{33} are very similar, both experimentally and theoretically. These trends are clearly reflected in the skew, κ, of the tensors. In comparing the experimental and theoretical data, one should keep in mind that they are obtained for different compounds, where the extremely large supermesityl substituent, in terms of theoretical calculations, has been replaced by H. Also, calculations are carried out for isolated gas-phase ions, rather than ionic solids. Nevertheless, the calculations faithfully reproduce the trends observed experimentally. Most importantly, the calculations confirm that the orientations of the phosphorus chemical shift tensors are similar for $H_2N-P═NH$, $[H_2N-P-NH_2]^+$, and $[H_2N-P-OH]^+$.

Interpretation of the Phosphorus Chemical Shielding Tensors. The close similarity of the ^{31}P chemical shift tensors for $RNH-P═NR$ and $[RNH-P-NHR]^+$ illustrates that the deshielding of phosphorus in phosphenium cations cannot be related to the formal positive charge on phosphorus. In order to gain a physical picture of the chemical shielding, it is helpful to refer to Ramsey's equations.[46] We have found this approach to be very useful in a previous study on the phosphinidene moiety in ruthenium carbonyl clusters.[47] In Ramsey's theory of magnetic shielding, the total shielding is made up of a diamagnetic term and a paramagnetic term. Trends in the chemical shifts among nuclei of any element other than hydrogen are generally rationalized by considering variations in the paramagnetic contribution to nuclear magnetic shielding. According to Ramsey's approach, the paramagnetic term for a nucleus A is

$$\sigma^{p}_{\alpha\beta} = -\frac{\mu_0}{4\pi}\frac{e^2}{2m^2}\sum_{k\neq 0}(E_k - E_0)^{-1}\left[\langle\Psi_0|\sum_i l_{i\alpha}|\Psi_k\rangle\left\langle\Psi_k\left|\sum_i \frac{l_{iA\beta}}{r_{iA}^3}\right|\Psi_0\right\rangle + \left\langle\Psi_0\left|\sum_i \frac{l_{iA\alpha}}{r_{iA}^3}\right|\Psi_k\right\rangle\langle\Psi_k|\sum_i l_{i\beta}|\Psi_0\rangle\right] \quad (1)$$

where μ_0 is the permeability of free space, e and m are electronic charge and mass, respectively, α and β refer to the Cartesian components (x, y, z), r_{iA} is the position vector for electron i, and l_{iA} is the electron angular momentum operator with respect to the observed nucleus A, whereas l_i is with respect to the chosen origin (*i.e.*, the gauge origin). Summations are taken over all electrons i and states k, except the ground state ($k = 0$), but including the continuum; E_k denotes the energy of the kth excited state.

While it is generally impossible to attribute variations in the shielding to any one term of eq 1, some general statements can

(46) Ramsey, N. F. *Phys. Rev.* **1950**, *78*, 699−703; **1952**, *86*, 243−246.
(47) Eichele, K.; Wasylishen, R. E.; Corrigan, J. F.; Taylor, N. J.; Carty, A. J. *J. Am. Chem. Soc.* **1995**, *117*, 6961−6969.

be made.[48] Because Ramsey's approach involves perturbation theory, the system in the presence of an external magnetic field is described by mixing excited states into the description of the ground state. Commonly, the ground- and excited-state molecular wave functions, Ψ_k, are approximated by high-lying bonding and low-lying antibonding orbitals, respectively. The mixing and hence the magnitude of σ^p will be larger as the energy separation between corresponding occupied and unoccupied orbitals decreases, resulting in greater deshielding. However, the energy difference serves only as a weighting factor. The electron angular momentum operators, l_i, ensure that mixing occurs only between orbitals related by magnetic dipole allowed transitions. Because they act as rotation operators, the magnitude of σ^p along a particular direction will depend on how efficiently l_i mixes orbitals in a plane perpendicular to the rotation axis.[49]

For an isolated atom, the paramagnetic term is zero for symmetry reasons, and the shielding behavior is controlled by the diamagnetic term. The shielding increases as the number of electrons about a nucleus increases. For example, the ^{31}P chemical shift of a *bare* phosphorus atom (P^{+15}) is 328 ppm, while the shift of the neutral free atom is -648 ppm and P^{3-} has a shift of -661 ppm.[50] In a linear molecule, the symmetry about the molecular axis is analogous to spherical symmetry and the paramagnetic term is zero for this direction. Therefore, high shielding is observed for the direction along the molecular axis. If this C_∞ symmetry axis is perturbed, *e.g.*, by a substituent, the paramagnetic term will also contribute to the magnetic shielding along the molecular axis. In Mes*C≡P[51] and $[Mes^*N{\equiv}P]^+$,[35] for example, the C_∞ symmetry is perturbed by the bulky substituent at carbon and nitrogen, respectively. Although this perturbation occurs remote from phosphorus, it induces a paramagnetic contribution of several hundred ppm to the direction along the E≡P bond. However, this direction is still highly shielded, $\delta_{33} = -273$ ppm, relative to the ^{31}P nuclei of most other phosphorus compounds.

A dramatic change in the nature of the chemical shift tensor occurs upon formation of the phosphenium cation. While the phosphorus chemical shift tensors of the first four compounds in Table 5 are characterized by high shielding along the molecular axis, those of the iminophosphine and the phosphenium cations are dominated by the deshielding observed along the direction of δ_{11}. Therefore, we shall limit our discussion to δ_{11} since it is this component of the ^{31}P chemical shift tensor that is responsible for the large chemical shifts of these species. As shown in Figure 5, δ_{11} is oriented within the molecular plane and perpendicular to the lone pair. Also depicted are the frontier molecular orbitals of $[H_2N{-}P{-}NH_2]^+$ and their relative ordering: π_1, lp, and π_2 are filled, with the nonbonding π_2 being the highest occupied MO (HOMO) and π_3 the lowest unoccupied MO (LUMO). According to the *ab initio* MO calculations, the nature of the frontier orbitals in the neutral $H_2N{-}P{=}NH$ is similar to those of the corresponding cation, except for the fact that the energies of all MO's in the latter are almost uniformly lower in energy due to the positive charge on phosphorus. From this picture, it is clear that rotation of the lone pair at phosphorus about the direction of δ_{11} will result in a very efficient overlap with π_3 and therefore the lp$\rightarrow\pi_3$ mixing is the most prominent single perturbation of the MO's induced by the external magnetic field. For the neutral iminophosphines, Gudat *et al.*[9] have shown that this lp$\rightarrow\pi_3$ mixing is the major cause of the deshielding of phosphorus. Our results demonstrate that the same interpretation can be applied to cationic species.

Energetically, mixing between HOMO and LUMO, $\pi_2\rightarrow\pi_3$, would be most favored. However, the π_2 orbital has a node at phosphorus, and therefore there is no contribution to σ^p from this mixing. Furthermore, as one reviewer pointed out, mixing between π orbitals parallel to one another should contribute little to σ^p.

Finally, we believe that the lack of a relationship between chemical shifts and charge is general.[52] In spite of many claims in the literature that shifts are related to charge, such arguments have no theoretical foundation.

Conclusions

A new and general mode of reactivity has been identified for the phosphadiazonium cation which involves nucleophilic attack at the phosphorus center, and the reaction is proposed to involve a σ-complex intermediate. Support for this mechanism is provided by the isolation and comprehensive characterization of $[Mes^*N{-}PPh_3][SO_3CF_3]$. Both observations are consistent with related chemistry of diazonium cations.[53] Finally, it is shown that the phosphorus shielding at dicoordinate phosphorus centers is not simply related to the formal charge at phosphorus. These conclusions are supported by model calculations. In these systems, paramagnetic contributions to magnetic shielding are significant and their interpretation requires consideration of the many contributions which control the phosphorus chemical shifts. For both the phosphenium centers and the neutral parent compounds, the deshielding of phosphorus originates from efficient mixing between the lone pair of electrons at phosphorus and the LUMO. This study also nicely demonstrates the powerful combination of solid-state NMR and *ab initio* MO calculations in developing an understanding of the anisotropic nature of chemical shielding.

Acknowledgment. We thank the Natural Sciences and Engineering Research Council of Canada for funding, the Atlantic Region Magnetic Resonance Centre for the use of instrumentation, Donna Silvert and Andrew McWilliams for preparation of some of the starting materials, and Professor Peter Pulay for the software necessary to perform the GIAO shielding calculations.

Supporting Information Available: Additional structural diagrams and listings of crystal data, positional parameters, bond lengths and angles, and anisotropic thermal parameters for **3**, **4**[$GaCl_4$], and **6**[SO_3CF_3] and an electron density map for **3** (27 pages). Ordering information is given on any current masthead page.

IC960131U

(48) (a) Saika, A.; Slichter, C. P. *J. Chem. Phys.* **1954**, *22*, 26−8. (b) Pople, J. A. *J. Chem. Phys.* **1962**, *37*, 53−59, 60−66. (c) Karplus, M.; Das, T. P. *J. Chem. Phys.* **1961**, *34*, 1683−92.

(49) (a) Jameson, C. J.; Gutowsky, H. S. *J. Chem. Phys.* **1964**, *40*, 1714−24. (b) Schatz, G. C.; Ratner, M. A. *Quantum Mechanics in Chemistry*; Prentice Hall: Englewood Cliffs, NJ, 1993; pp 92−95.

(50) Saxena, K. M. S.; Narasimhan, P. T. *Int. J. Quantum Chem.* **1967**, *1*, 731−749.

(51) Duchamp, J. C.; Pakulski, M.; Cowley, A. H.; Zilm, K. W. *J. Am. Chem. Soc.* **1990**, *112*, 6803−6809.

(52) (a) Grutzner, J. B. In *Recent Advances in Organic NMR Spectroscopy*; Lambert, J. B., Rittner, R., Eds.; Norell Press: Landisville, NJ, 1987. (b) Kutzelnigg, W.; van Wüllen, C.; Fleischer, U.; Franke, R.; v. Mourik, T. In ref 42b, pp 141−161.

(53) Reference 2, Vol. 1, pp 214−230.